Received: 18 February 2021 | Revised: 21 July 2021 | Accepted: 1 September 2021

DOI: 10.1002/joc.7382

RESEARCH ARTICLE

International Journal of Climatology RMetS

Dynamical-statistical long-term prediction for tropical cyclone landfalls in East Asia

So-Hee Kim[1] | Joong-Bae Ahn[2] | Jianqi Sun[3]

[1]Department of Atmospheric Sciences, BK21 School of Earth and Environmental Systems, Pusan National University, Busan, South Korea

[2]Department of Atmospheric Sciences, Pusan National University, Busan, South Korea

[3]Nansen-Zhu International Research Centre (NZC), Institute of Atmospheric Physics, Chinese Academy of Sciences, Beijing, China

Correspondence

Joong-Bae Ahn, Department of Atmospheric Sciences, Pusan National University, 2, Busandaehak-ro 63beon-gil, Geumjeong-gu, Busan, South Korea.

Email: jbahn@pusan.ac.kr

Funding information

Cooperative Research Program for Agriculture Science & Technology Development, Grant/Award Number: PJ01489102

Abstract

This study develops a statistical-dynamical seasonal typhoon forecast model (SDTFM) that utilizes the statistical correlation between East Asia (EA) tropical cyclone (TC) landfall and atmospheric circulation predicted by a coupled general circulation model for seasonal prediction and its predictability is verified. A total of 40 ensemble members produced through different data assimilation and time-lag methods introduced as a way to reduce the initial condition error and model uncertainty enabled the development of the new SDTFM. According to the results, the SDTFM developed in this study showed significant predictability in TC landfall prediction when using the month of May for the initial conditions for the entire East Asia (EEA) and its three subdomains: Northern East Asia (NEA), Middle East Asia (MEA), and Southern East Asia (SEA). The predicted TC season is July–September (JAS), and only for SEA, including South China, the Philippines, and Vietnam, it is July–November (JASON) considering the relatively long landfall period. The models developed for each domain significantly predict the interannual variability of TC landfall at the 99% confidence level. The cross-validated results are still significant at the 99% confidence level in NEA and SEA and the 95% confidence level in MEA and EEA.

KEYWORDS

CGCM, seasonal prediction, statistical-dynamical model, tropical cyclones (TCs), typhoons landfall

1 | INTRODUCTION

Tropical cyclone (TC) is a rapidly rotating storm system that develops by obtaining energy from warm tropical ocean. It is called typhoons (in the Western North Pacific), hurricanes (in the Atlantic and Eastern North Pacific) or cyclones (in the South Pacific and Indian Ocean) according to the area of occurrence, and are accompanied by hazardous weather, including strong winds and heavy rains. In recent years, strong TCs are frequently occurring, such as Haiyan in 2013 and Meranti in 2016, which have caused serious damage in East Asia (Mori and Takemi, 2016). In particular, Haiyan that made landfall in the Philippines is one of the strongest TCs ever recorded in the region, classified as a Category 5 storm on the Saffir-Simpson hurricane wind scale. East Asia resides more than 20% of the world's population, making it more vulnerable to extreme weather such as

TCs. Moreover, climate change could make the damage caused by TC more severe. Tu *et al*. (2009) showed that TC activity near Taiwan increased from 3.3 per year before 2000 to 5.7 per year after 2000 during the period from 1970 to 2006. Park *et al*. (2011) showed that the number of EA TCs that make landfall will increase as the TC season lengthens, and the precipitation and the Power Dissipation Index (PDI), defined as the sum of the maximum one-minute sustained wind speed cubed when the cyclone is at least of tropical storm strength, will increase significantly in the future. In addition, rising sea levels due to climate change is particularly adding to the damage caused by TCs that make landfall (IPCC, 2014, 2019). Therefore, reliable seasonal predictions of East Asia (EA) TCs that make landfall will help prevent and minimize various types of damage by preparing for them in advance.

Despite the importance of seasonal predictions about TCs, due to the complex and chaotic nature of a TC's occurrence and development, it is difficult to predict its generation, size, intensity, and track, even just a few days ahead. The first type of attempt at seasonal predictions of EA TCs that will make landfall is a statistical method that uses atmospheric and ocean initial conditions as predictors before the onset of the TC season (Chan *et al*., 1998; Chan *et al*., 2001; Fan and Wang, 2009). However, this method is vulnerable to climate variations, such as inter-annual and decadal variations, because it is based on the assumption that statistical relationships will be valid for the next season and beyond (Vitart and Stockdale, 2001). Since the 2000s, with the development of the Coupled General Circulation Model (CGCM), it has been possible to use dynamic methods to predict TC frequency and movement. However, despite the continuous development and improvement of the model, our poor understanding of the physical processes associated with TCs, and the sparse spatial resolution of the dynamic models, make TC-related predictions difficult (Zhang *et al*., 2017). Moreover, as the lead time increases, the prediction ability of the dynamic models becomes lower because the influence of the initial conditions decreases as well.

However, the dynamic models generally have a meaningful ability to predict large-scale environmental variables, such as vertical shear and the low-level vorticity closely related to TCs. Therefore, many researchers have paid attention to the relationship between large-scale environmental variables produced by a dynamic model and observed predictands (e.g., the frequency of, or landfalls made by, TCs) using statistical methods such as linear regression and Poisson regression, and have attempted to predict TCs by utilizing the relationship. Such hybrid models called a statistical-dynamical seasonal typhoon forecast model (SDTFM) are often used for seasonal prediction of the track (Liu and Chan, 2003; Sun and Ahn, 2011; Wang *et al*., 2013; Zhang *et al*., 2013, 2016, 2017) and the frequency (Chan *et al*., 1998; Fan, 2007, 2010; Fan and Wang, 2009; Wang *et al*., 2013; Zhang *et al*., 2013, 2016; Kim *et al*., 2017) of EA TCs that make landfall, as well as Atlantic TCs that make landfall (Vitart and Stockdale, 2001; Zhao *et al*., 2010; Vecchi *et al*., 2011; Vecchi and Villarini, 2014; Camp *et al*., 2015; Xiang *et al*., 2015).

The predictability of an SDTFM generally depends on how well the used dynamic model predicts the predictors (Vecchi *et al*., 2011; Li *et al*., 2013; Kim *et al*., 2015; Murakami *et al*., 2016; Zhang *et al*., 2017). However, it is also important to select appropriate predictors to develop an effective SDTFM, because a prediction based on the physical correlation between predictand and predictor is relatively stable (Zhang *et al*., 2017). Therefore, it is necessary to analyse the correlation between landfalling TCs (LTC) and large-scale atmospheric variables. The damage caused by TCs is more related to their storm tracks than to where and how often they occur, so this study focuses on predicting TC tracks. In this regard, several previous studies have shown that the flow in the lower and middle troposphere (700 hPa and 500 hPa) significantly affects the movement of EA TCs (Chan and Gray, 1982; Harr and Elsberry, 1991, 1995). Based on those, this study intends to use the atmospheric circulation predicted by the CGCM for the prediction of TC landfalls in each domain.

Sun and Ahn (2011) previously developed an SDTFM for the period 1979–2009 using v1.0 of the Pusan National University (PNU) CGCM, which is a participation model of the Asia Pacific Economic Cooperation (APEC) Climate Center multi-model ensemble (APCC MME) prediction system. However, the SDTFM developed by them only predicts LTCs in South China. This study develops a new SDTFM for LTCs that influence all East Asian countries by using PNU CGCM v2.0. Unlike v1.0, PNU CGCM v2.0 utilizes ocean data assimilation and produces a total of 40 ensemble members for each month by using time-lag methods. Extended ensemble members reduce the error in initial conditions as well as in the model uncertainty (Weigel *et al*., 2008), enabling the development of a new SDTFM for EA TC landfalls.

Section 2 describes the CGCM, the data, and the predicted domains and TC season used in this study, and Section 3 analyses the relationship between atmospheric circulation and TC landfall for each domain. Section 4 examines the possibility that the PNU CGCM can be developed as an SDTFM based on the relationships discussed in Section 3. In Section 5, the SDTFM is developed using PNU CGCM v2.0 and linear regression, and the predicted results are verified. Section 6 compares the model developed in this study with other models, and Section 7 presents a summary and a conclusion to the study.

2 | MODEL AND DATA

2.1 | The coupled general circulation model

The CGCM utilized in this study (PNU CGCM v2.0) is one of the participating models of the Long-range Multi-model Ensemble (LR-MME) prediction system of the APCC (Jeong *et al.*, 2008; Ahn *et al.*, 2012). The PNU CGCM forecast data of eight-month leads with 40 ensemble members are provided to the APCC each and every month. The ocean data assimilation (ODA) is used when initial conditions of each ensemble member are produced. A total of 40 ensemble members is large enough to minimize the initial conditions error and model uncertainty, considering the number of ensemble members produced by global institutes producing long-term predictions using state-of-the-art CGCMs. The details and performance of the model were introduced and studied by several authors (Ahn and Kim, 2014; Jo and Ahn, 2015; Bayasgalan and Ahn, 2018).

The ensemble prediction ability of the model depends on the ensemble method used, as well as the number and features of the ensemble members (Oh and Suh, 2017; Seong *et al.*, 2017). The method used in this study is a simple composite method (SCM) that arithmetically averages each ensemble member. The method is widely used because it is simple and has relatively better predictability compared to other sophisticated methods (Min *et al.*, 2014; Ahn and Lee, 2016; Kim *et al.*, 2021).

2.2 | The data

Observed TC data used in this study are the best track data from the Regional Specialized Meteorological Center (RSMC) Tokyo, which are widely used in TC research in Asia (Sun and Ahn, 2011; Choi *et al.*, 2015; Zhang *et al.*, 2017). TCs in Western North Pacific are classified into tropical depression (~33kt), tropical storm (~47kt), severe tropical storm (~64kt), and typhoon (64kt~) according to the maximum wind speed averaged over 10 min. In this study, EA LTCs included tropical storms, severe tropical storms, and typhoons that affected the domain. It is because, although a tropical storm is not generally stronger than a typhoon, it still causes great damage. The monthly average atmospheric variables, such as horizontal wind and relative vorticity, from the National Centers for Environmental Prediction of the Department of Energy (NCEP-DOE) Re-analysis 2 (R-2) are used to analyse the atmospheric circulation related to EA TC landfalls (Kanamitsu *et al.*, 2002). The horizontal resolution of the re-analysis data is 2.5°× 2.5° with 17 vertical levels spanning January 1979 to the present.

2.3 | Forecast region and period

The research domain covers the whole of EA because LTCs cause damage across all regions of EA. The TC tracks that determine the landing area in EA are all different for each TC and can be divided into three types (Figure S1). This means that regional prediction of TC landfall is possible through atmospheric circulation affecting each type of TC track. Therefore, the forecast region was subdivided into three climatically similar regions (Chan and Xu, 2009; Huang and Chan, 2014; Zhang *et al.*, 2017). The domains located 30°N to 40°N and 124°E to 143°E includes the Korean Peninsula and Japan, 22°N to 40°N and 117°E to 124°E includes Taiwan, Fujian, Zhejiang, Jiangsu, and Shanghai, and 5.7°N to 23.5°N and 117°E to 127°E includes South China, Vietnam, and the Philippines. The entire East Asia (EEA) comprises Northern East Asia (NEA), Middle East Asia (MEA), and Southern East Asia (SEA), as marked in Figure 1. In this study, if a TC passes through one domain, it is regarded as a TC making landfall in the domain. If a TC passes through more than one domain, it is assumed that all those domains are affected by the

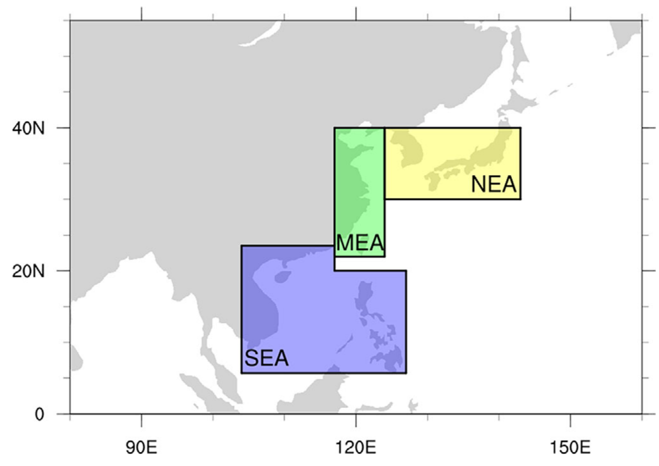

FIGURE 1 Sub-domains used to define tropical cyclones (TCs) making landfall in East Asia. The domains located 30°N to 40°N and 124°E to 143°E, 22°N to 40°N and 117°E to 124°E, and 5.7°N to 23.5°N and 117°E to 127°E are northern East Asia (NEA), Middle East Asia (MEA), and southern East Asia (SEA), respectively. Entire East Asia (EEA) contains all three sub-domains [Colour figure can be viewed at wileyonlinelibrary.com]

TC. Moreover, the subdivision of the forecast region is appropriate to simulate different regional trends in EA TC activity (Lee *et al*., 2012).

The research period for this study is from 1980 to 2018. Figure 2 shows the average monthly landfall frequency of EA TCs and typhoons for each domain. For NEA, MEA, and EEA, 73% (81%), 76% (79%), and 59% (63%) of the total annual TCs (typhoons) land from July–August–September (JAS), respectively. This period during which most of the total annual landfalls occur is defined as the predicted TC season for these domains. For SEA, a TC lands at least once a month from May to November, which is longer than the other domains. In particular, in July–August–September–October–November (JASON), typhoons land relatively frequently, so it is defined as SEA TC season. During this period, 72% (78%) of the total annual TCs (typhoons) land on SEA. In addition, atmospheric circulation used in this study is averaged during each TC season for each domain.

3 | RELATIONSHIP BETWEEN EA TC LANDFALLS AND ATMOSPHERIC CIRCULATION

In order to use mid- and low-level atmospheric circulation as a predictor, the relationship with TC landfalls for each domain is examined using the relative vorticity and horizontal wind at 700 hPa and 500 hPa. Figure 3 presents a regression of the relative vorticity and horizontal wind in the re-analysis data for NEA LTCs, which show favourable atmospheric circulation for TC to land in NEA. Figure 3a,c shows the NEA vorticity pattern at 500 hPa (700 hPa), and Figure 3b,d shows the NEA wind pattern at 500 hPa (700 hPa). P (N) in the NEA vorticity patterns indicate the centre of positive (negative) vorticity, and the solid (dashed) lines indicate the positively (negatively) significant areas at 95%, 98%, and 99% confidence levels. Shading in the NEA wind patterns also indicates an area at the 95% confidence level. The NEA vorticity patterns consist of a negative vorticity over the Korean Peninsula, and positive vorticities over east China and the tropical Pacific (see Figure 3a,c). The negative vorticity over the Korean Peninsula and the positive vorticity over the tropical Pacific are more evident and significant at 700 hPa (Figure 3c) than at 500 hPa (Figure 3a), but the overall patterns in both layers are similar. The regression patterns indicate atmospheric circulation in support of TC landfalls, and previous studies allow understanding of the patterns.

On both the interannual and interdecadal timescale, the western North Pacific subtropical High (WNPSH) can have a significant impact on the EA TC activities (Choi and Moon, 2012; Wang *et al*., 2013). Therefore, composite

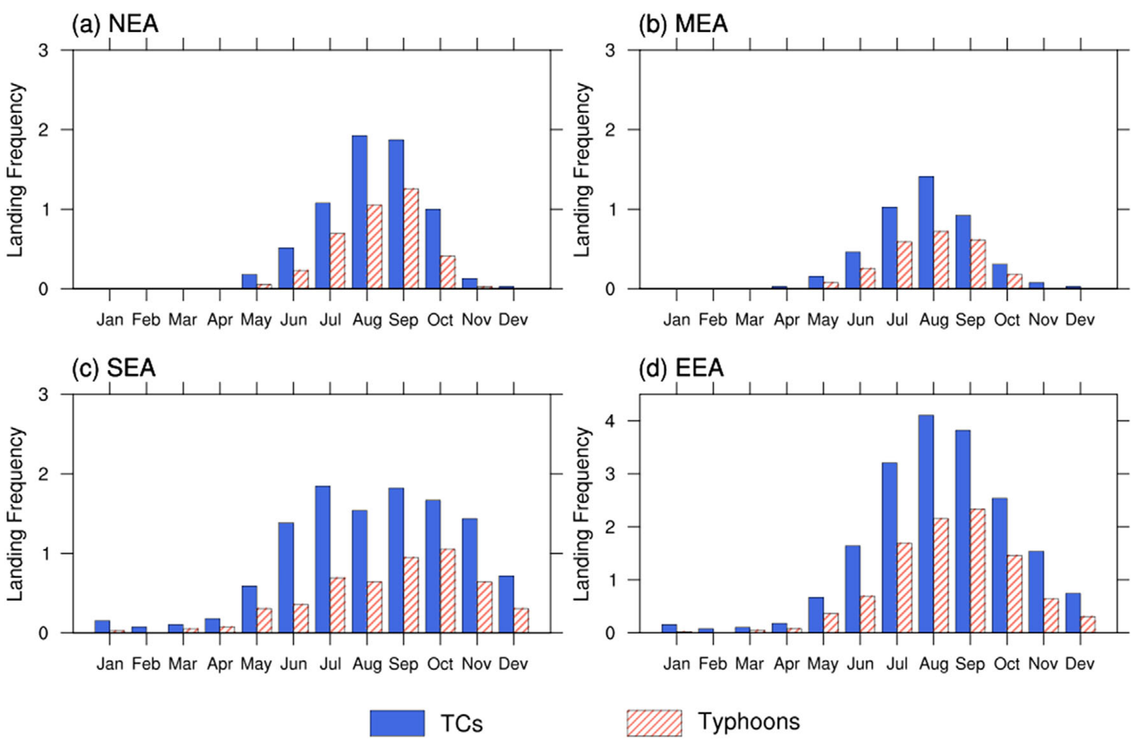

FIGURE 2 Average monthly landfall frequency of TCs and typhoons from 1980 to 2018 in (a) NEA, (b) MEA, (c) SEA, and (d) EEA. The TCs include tropical storms, severe tropical storms, and typhoons [Colour figure can be viewed at wileyonlinelibrary.com]

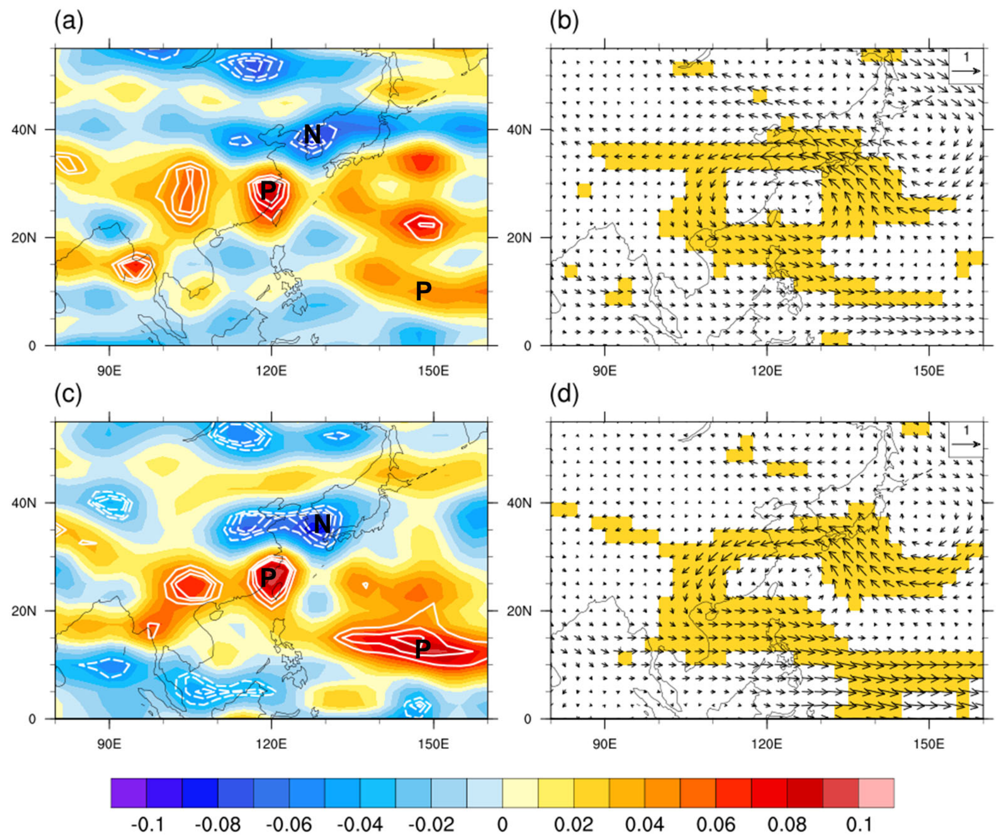

FIGURE 3 Regression of (a) relative vorticity and (b) horizontal winds at 500 hPa from re-analysis 2 (R-2) against the observed TC landfalls over NEA for 1980–2018; (c) and (d) are the same as (a) and (b), but at 700 hPa. P (N) in (a) and (c) indicate the positive (negative) vorticity centre, and the solid (dashed) lines indicate positively (negatively) significant areas at the 95%, 98% and 99% confidence levels. Shading in (b) and (d) indicates the areas at the 95% confidence level [Colour figure can be viewed at wileyonlinelibrary.com]

TABLE 1 The years in which TCs made landfall at above- and below-normal levels over NEA, MEA, SEA and EEA

Domain	Above-normal years (AN_Years)	Below-normal years (BN_Years)
NEA	1991, 1993, 2000, 2002, 2012, 2018	1980, 1981, 1983, 1984, 1995, 2003, 2008, 2009, 2013, 2017
MEA	1994, 2000, 2005, 2006, 2012, 2015, 2018	1983, 1986, 1988, 1993, 1995, 1999, 2009, 2011, 2014, 2017
SEA	1983, 1994, 1995, 2013, 2017	1982, 1999, 2002, 2004, 2010, 2011, 2014, 2015
EEA	1991, 1994, 2000, 2002, 2018	1980, 1981, 1983, 1984, 1986, 1998, 2003, 2008, 2014

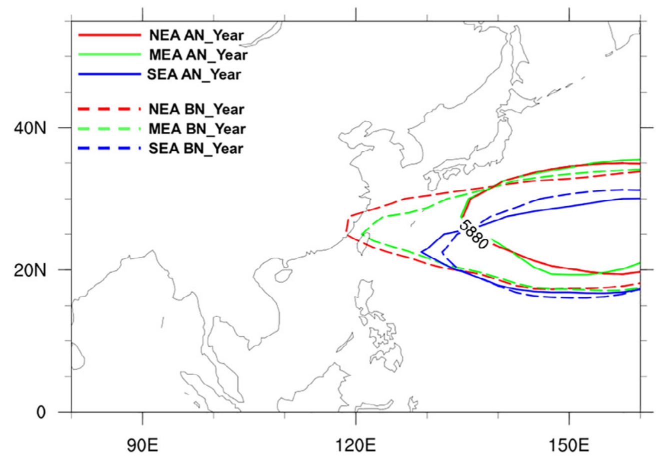

FIGURE 4 Composite of 5,880 gpm lines empirically representing the summer Western North Pacific high at 500 hPa in the above-normal years (AN_years) (solid line) and the below-normal years (BN_Years) (dashed line) over NEA, MEA and SEA [Colour figure can be viewed at wileyonlinelibrary.com]

analysis was conducted to examine the effects of WNPSH on TC landfalls for each domain. The years in which the landfall frequency deviates from the normal range ($-1\sigma \sim +1\sigma$) are defined as above-normal years (AN_Years) or below-normal years (BN_Years) and are summarized in Table 1. Figure 4 shows 5,880 gpm lines at 500 hPa during the AN_Years (solid) and BN_Years (dashed), which empirically represent the boundary of the summer WNPSH. In the NEA BN_Years, the WNPSH expanded in the zonal direction, while it contracted in the NEA AN_Years. This means that the contraction of WNPSH could be related to the positive vorticity over east China shown in the NEA vorticity patterns (Figure 3a,c). The positive vorticity together with the negative vorticity over the Korean Peninsula constitutes a dipole pattern, which is analogous to the positive Pacific-Japan (PJ) teleconnection pattern. In this regard, previous studies showed that TCs land more frequently on NEA when the PJ pattern is positive than negative (Choi *et al*., 2010a; Kim *et al*., 2012). Kim *et al*. (2012) also reported that during the negative PJ pattern, the WNPSH expands in the zonal direction (like NEA BN_Years in Figure 4), which prevents TCs from taking a northeastward track.

The significant positive vorticity over east China produces an anomalous cyclonic flow (Figure 3b,d). In particular, the negative vorticity over the Korean Peninsula contributes to the TC landfall into NEA by strengthening anomalous southeasterlies over the Korean Peninsula and the south of Japan. In addition, the contradicting flows between the subtropics and tropics can generate cyclonic wind shears and positive vorticity in the lower troposphere (Harr and Elsberry, 1995; Chu *et al*., 2007). This atmospheric circulation favours TC generation and prevents TCs from entering SEA by affecting the low-level vorticity and vertical wind shear, allowing more TCs into NEA (Choi *et al*., 2010b). Meanwhile, the NEA wind pattern is associated with the strong Western North Pacific (WNP) monsoon. Wang and Fan (1999) found that strong convection of the WNP monsoon induces anomalous cyclonic flow, which is a circulation condition favourable for TC generation. Wang and Chan (2002) and Choi *et al*. (2015) showed that when the WNP monsoon is strong, TCs generated in the eastern part of the WNP frequently move towards NEA. Choi *et al*. (2015) also showed a positive correlation between the WNP monsoon index defined by Wang and Fan (1999) and LTCs in Korea.

The positive vorticity in the tropical Pacific, the other major component of the NEA vorticity pattern, could be associated with Madden-Julian oscillation (MJO). Kim *et al*. (2008) examined the variability of TC activities according to the MJO category and found that the MJO-related convection centre is strongly related to NEA LTCs. They showed that when the convection occurs in the tropical Pacific, TCs occur more and have northward tracks because of the influence of the monsoon trough enhanced by the anomalous westerlies. Thus, the regressed circulation shown in Figure 3 can be regarded as the characteristic pattern at the middle and lower levels associated with TCs making landfall in NEA.

Figure 5 shows the relative vorticity and the horizontal wind from the re-analysis data regressed onto TC landfalls in MEA. The regressed vorticities are similar regardless of the level, which show that MEA LTCs strongly correlate with mid- and low-level atmospheric circulation. The MEA vorticity patterns consist of negative vorticities from east China to the east of Japan and positive vorticities from the Indochina Peninsula to the North Pacific (Figure 5a,c). This dipole pattern causes distinctly contradicting wind anomalies in subtropics and

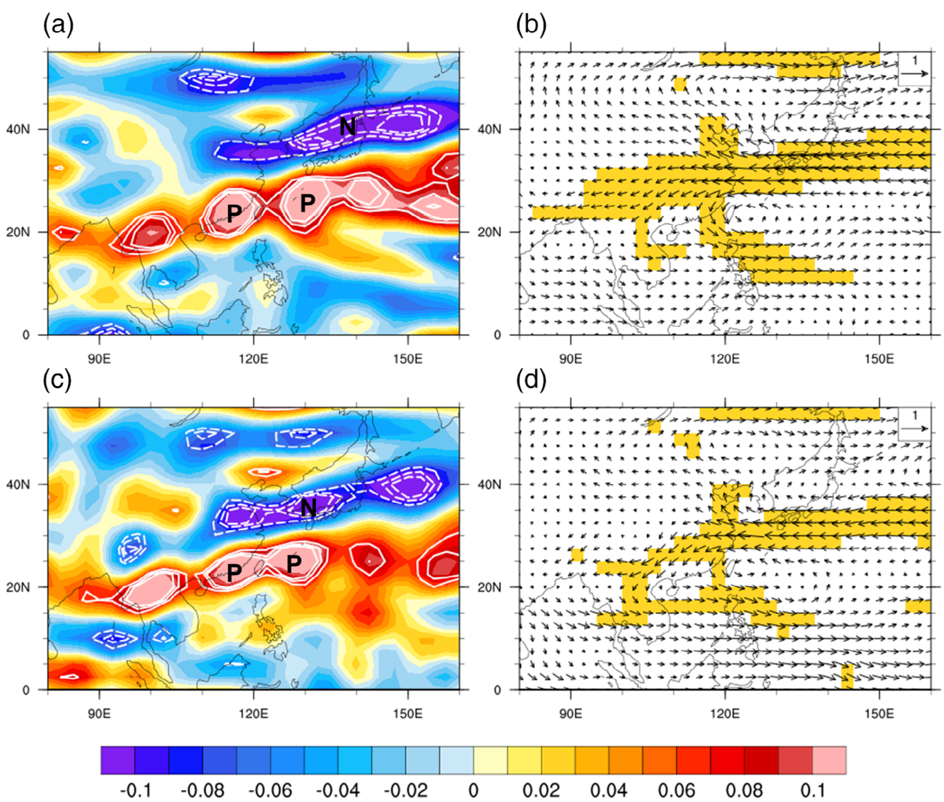

FIGURE 5 As in Figure 3, but for TC landfalls over MEA [Colour figure can be viewed at wileyonlinelibrary.com]

tropics, aiding landfalls into the MEA (Sparks and Toumi, 2021). In Figure 4, the contracted WNPSH enables frequent landfall on MEA. These characteristics are similar to those shown in the NEA pattern, but there are important (albeit small) differences that determine the landing area. The latitude at which the anomalous easterlies shown in the NEA wind pattern is 30°N to 40°N, while it is 25°N to 35°N in the MEA wind pattern. Before landing on NEA, the strong anomalous easterlies at 25°N to 35°N make TCs land on MEA, and the weakened TCs are mostly extinct without propagating to NEA. In contrast, the anomalous easterlies at 30°N to 40°N allow TCs to land in NEA without dissipation. Owing to this difference, only 14 TCs have passed both sub-domains in 39 years, which is extremely low compared to 153 NEA LTCs and 101 MEA LTCs. In addition, the MEA vorticity patterns do not show the positive vorticity associated with MJO in the tropical Pacific. Therefore, the NEA and MEA patterns are clearly different, and the circulation pattern shown in Figure 5 represents the atmospheric circulation associated with MEA landfalls (especially the steering flow).

Figure 6 shows the regression of the relative vorticity and the horizontal winds of the re-analysed data onto TC landfalls in SEA. The main features of the SEA vorticity pattern at both levels are similar and are relatively more significant at 700 hPa. The patterns consist of positive vorticity over the sea near the Korean Peninsula, negative vorticities near 25°N, and positive vorticities near 15°N (Figure 6a,c). The significant anomalous northwesterlies over Japan shown in the SEA wind patterns are related to the positive vorticity over the sea near the Korean Peninsula, which means a lack of flow to help a TC propagate to the mid-latitudes (Figure 6b,d). The vorticity pattern in the mid-latitudes is relatively insignificant compared to other sub-domains (Compared with Figures 3 and 5), which could result from the weak relationship between SEA LTCs and WNPSH. In this regard, Figure 4 shows that for SEA, the difference in the development of WNPSH during the AN_Years and BN_Years is negligible. On the other hand, the positive vorticities near 15°N are favourable for the generation of TCs, increasing the likelihood of landfall in SEA. The positive vorticities with negative vorticities near 25°N induce anomalous easterlies near 20°N, which is the steering flow that lands TCs into SEA. Meanwhile, this wind pattern is associated with a weak summer monsoon trough. Wang and Chan (2002) and Choi *et al.* (2015) showed that when the WNP monsoon is weak, TCs in the western part of the WNP frequently made landfall in SEA. Thus, the patterns shown in Figure 6 contain atmospheric circulations specific to frequent SEA TC landfalls.

Figure 7 shows the regression between relative vorticity and horizontal winds with TC landfalls in EEA. The EEA vorticity patterns (Figure 7a,c) are composed of negative vorticities around 40°N, positive vorticities around

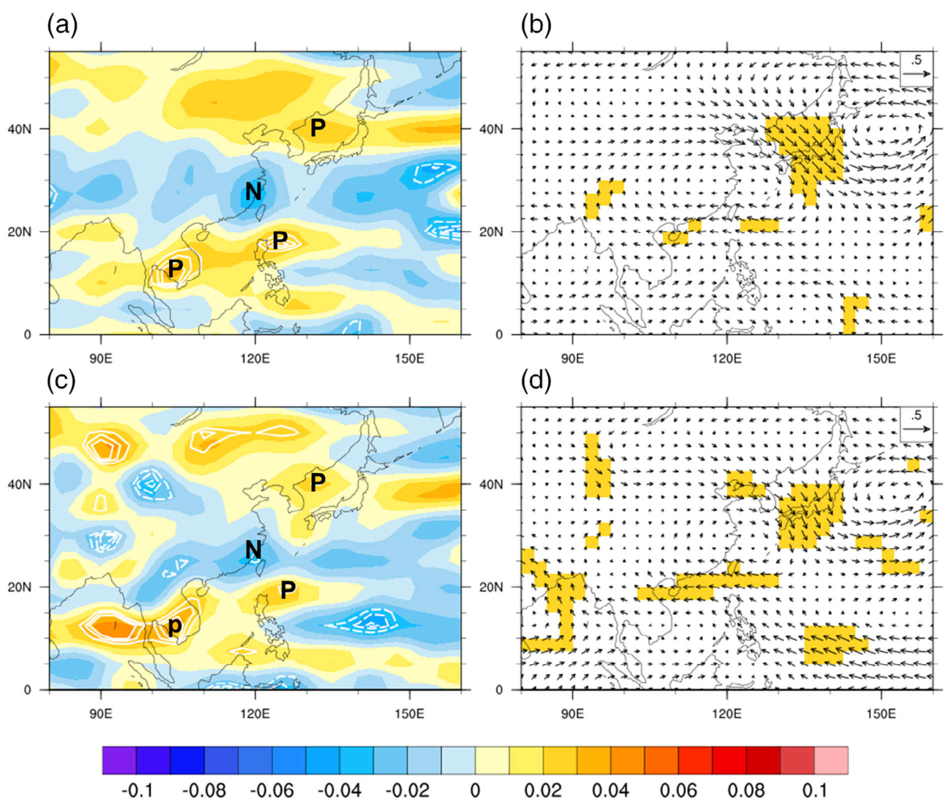

FIGURE 6 As in Figure 3, but for TC landfalls over SEA [Colour figure can be viewed at wileyonlinelibrary.com]

20°N, and negative vorticity near the equator. The negative vorticities around 40°N expand further zonally at 500 hPa and the negative vorticity near the equator is more significant at 700 hPa, but the overall phases of the pattern in both layers are similar. The EEA vorticity patterns induce the EEA wind patterns, including the strong anomalous westerlies in the tropics, and the anomalous easterlies in the subtropics. In these patterns, the main features of the NEA and MEA patterns are captured together. Although SEA landfalls occur most frequently compared to landfalls in other regions, the weak wind pattern of SEA is masked by the strong wind patterns of NEA and MEA. This suggests that one forecast region covering all of EA smooths out the unique circulation characteristics associated with TC landfalls on each subdomain. This could result in erroneous predictions, so the subdivision of the forecast region in this study is reasonable.

4 | POSSIBILITY OF PREDICTING TC LANDFALLS USING PNU CGCM V2.0

The prediction ability of the dynamic model is crucial to determining successful SDTFM development (Vitart and Stockdale, 2001). From that perspective, the predictability of PNU CGCM v2.0 for the atmospheric circulation discussed in Section 3 is evaluated. However, it is relatively difficult to predict the atmospheric circulation at the mid and low levels used as predictors, compared to other meteorological elements. That is because low-level wind is strongly influenced by surface processes, which are extremely complex and difficult to understand due to the inhomogeneous and turbulent nature of the surface boundary flows. Such conditions make it difficult to parameterize these processes, resulting in great error in wind simulated according to local influences. The turbulent variations of the wind are eliminated in this study by using monthly averaged data. Evaluating the similarity of temporal variations at each grid point is a general method of predictability evaluation, but it is not appropriate in this study related to large-scale circulation (Lee *et al.*, 2016). Thus, we focused on whether the CGCM similarly predicts relative vorticity and horizontal wind related to the TC landfalls. This study evaluates predictability based on atmospheric circulation discussed in Section 3, and then develops the SDTFM.

The hindcast data needed for regression between predicted relative vorticity and observed TC landfalls are the output from model integration with the January (six-month to eight-month) to June (one-month to three-month) initial conditions. Of the seven-month initial conditions, the May initial conditions (two-month to six-month) were used because its regression results were stable for all domains. Since the regression of predicted

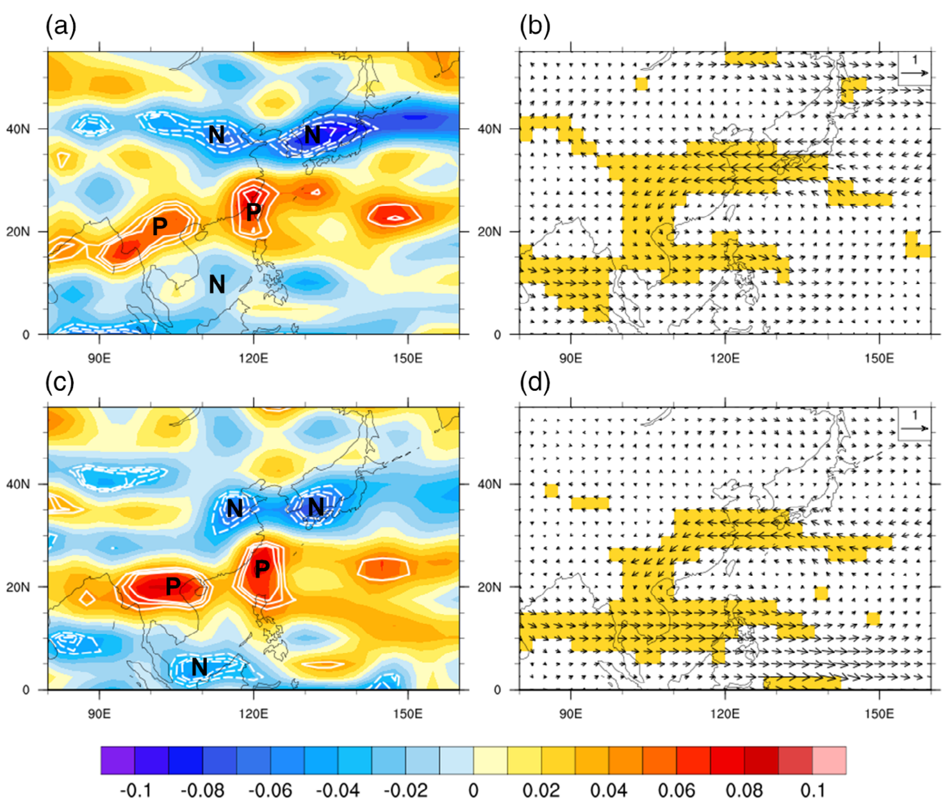

FIGURE 7 As in Figure 3, but for TC landfalls over EEA [Colour figure can be viewed at wileyonlinelibrary.com]

atmospheric circulation for observed TC landfalls is more significant at 700 hPa only in MEA (not shown), atmospheric circulation at 700 hPa is used as a predictor only in MEA. In this regard, we have already seen in Section 3 that the patterns associated with TC landfalls at 500 hPa and 700 hPa are similar for each domain. Therefore, we select the layer that PNU CGCM predicts more significantly and compare it with the regression pattern using re-analysis data at the same layer.

Figure 8 shows the regression between the relative vorticity predicted by PNU CGCM v2.0 and the observed TC landfalls for each domain. P (N) indicate the centre of positive (negative) vorticity, and the dashed lines indicate the significant areas at the 95%, 98%, and 99% confidence levels. In Figure 8a, the positive vorticities over east China and the tropical Pacific shown in the NEA vorticity pattern appear similar, but the negative vorticity shifts to the north of Japan. Figure 8b shows that the positive vorticity centre shown in the MEA vorticity pattern appears similar, but the negative vorticity shifts to the north of Japan. In Figure 8c, the positive vorticity over the Korean Peninsula and Japan shown in the SEA vorticity pattern appears similar, but the other vorticities are shifted relatively south. The negative vorticities near 25°N shift to 15°N and the positive vorticity near 15°N shifts to 5°N. Figure 8d for EEA shows that the two negative vorticities around 40°N, shown in the EEA vorticity pattern, shift to central China and Japan, respectively. However, the positive vorticities around 20°N and the negative vorticity near the equator maintain similar positions. Considering these results, PNU CGCM v2.0 is sufficiently developable as SDTFM because it can significantly predict the unique characteristics of the circulation discussed in Section 3.

5 | THE STATISTICAL-DYNAMICAL SEASONAL TYPHOON FORECAST MODEL

Regarding predictors for SDTFM development, Wilks (2006) reported that many predictors in multivariate regression do not necessarily give better predictability because of overfitting problems. In particular, the model in this study is based on simultaneous relationships and therefore does not require as many predictors as those based on lagged relationships (Wang *et al.*, 2009). Sections 3 and 4 suggest that the vorticities in the boxed regions in Figure 8 have a significant impact on the TC landfalls for each domain. Thus, they are defined as potential predictors for each domain and are summarized in Table 2. x_1 and x_2 for NEA are associated with steering flow and MJO, respectively, and those for MEA only relate to steering flow. In this regard, Sparks and

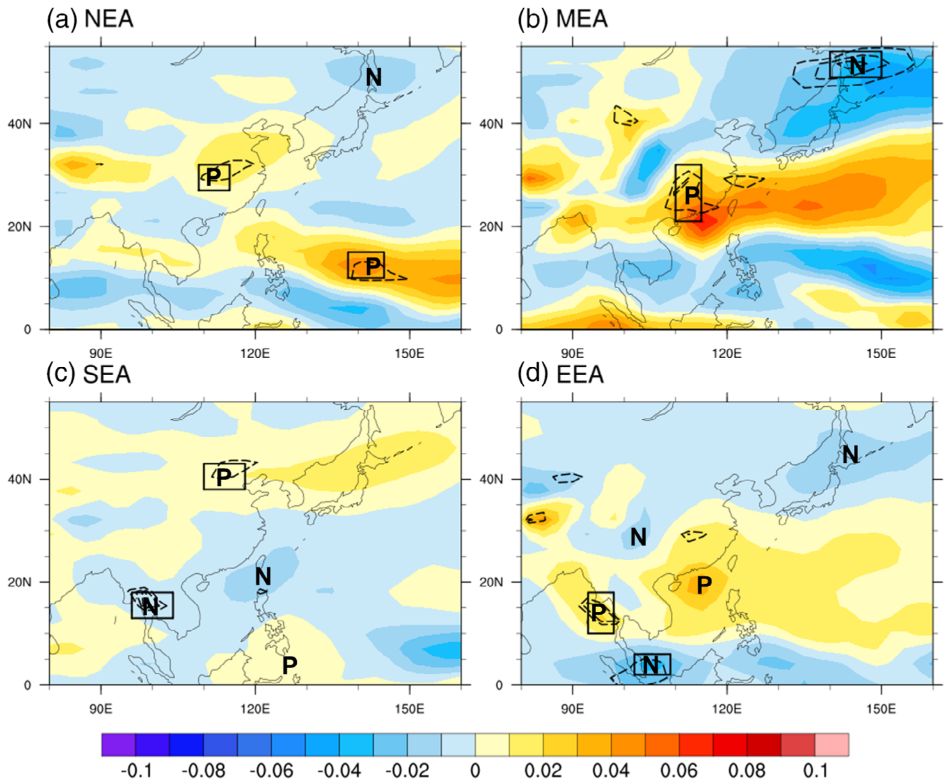

FIGURE 8 Regression of relative vorticity at (a) 500 hPa, (b) 700 hPa, (c) 500 hPa, and (d) 500 hPa from the PNU coupled general circulation model (PNU-CGCM) onto the observed TCs over (a) NEA, (b) MEA, (c) SEA, and (d) EEA for 1980–2018. The dashed lines indicate significant areas at the 95%, 98%, and 99% confidence levels. P (N) indicates the centres of positive (negative) vorticity, and boxes are the areas selected as potential predictors [Colour figure can be viewed at wileyonlinelibrary.com]

Toumi (2021) showed a negligible correlation between the MEA landfall frequency and large environmental climate indices (PMM, El-Nino, and PDO, etc.). They emphasized the importance of steering flow in landfall prediction for MEA. x_1 for SEA makes it difficult for a TC to enter the mid-latitudes, and x_2 helps a TC enter SEA with frequent TC generation and distinct steering flow (albeit weak). The potential predictors of EEA are also associated with frequent TC landfalls in terms of their occurrence and steering flow.

For each domain, the regression was repeated for three cases of predictors, and the best-case was determined by comparing the results. Of the three cases, the first uses only x_1 as predictor, the second uses only x_2, and the third uses x_1 and x_2 together. The method used was the same as Kim *et al*. (2017), which selected one or two predictors from the potential predictors depending on the initial conditions. The goodness-of-fit measures were used to minimize the root mean squared errors (RMSE), and maximize the coefficient of determination (R^2) and the *F*-ratio (Wilks, 2006). Table 3 summarizes the results for each case of predictors, where the best-case is the third case (x_1 and x_2) for NEA and SEA, the second case (x_2) for MEA, and the first case (x_1) for EEA, respectively. Finally, Table 4 lists the SDTFMs developed with the best-case of predictors. All regression equations are significant with *p*-values up to 0.006 in the *F*-test. Each regression coefficient is significant at the 99.9% confidence level using the student's *t*-statistic.

Figure 9 shows the time series of observed TC landfalls, TC landfalls predicted with the SDTFM, and cross-validated TC landfalls for the 39 years from 1980 to 2018. Leave-One-Out Cross-Validation (LOOCV) was applied to verify the SDTFM (Sun and Ahn, 2011). SCOR and FCOR are the correlation coefficients of the observed TC landfalls with the predicted and cross-validated TC landfall, respectively. The SCOR for NEA, MEA, SEA, and EEA were 0.583, 0.427, 0.570, and 0.449, respectively, which were significant at the 99% confidence level. The FCOR for NEA, MEA, SEA, and EEA were 0.445, 0.343, 0.463, and 0.339, respectively. They are significant at the 99% confidence level for NEA and SEA and 95% confidence level for MEA and EEA. These results mean that the developed SDTFM can be used effectively to predict TC landfalls.

To further evaluate the SDTFM, the relative vorticity and horizontal wind in the re-analysis data regress onto predicted TC landfalls (Figure 10). The solid (dashed) lines in the left column indicate the positively (negatively) significant areas at the 95%, 98%, and 99% confidence levels, and shading in the right column is significant for the 95% confidence level. Figure 10a shows the main characteristics of the NEA vorticity pattern (Figure 3a) (e.g., negative vorticity over the Korean Peninsula and positive vorticities over east China and tropical Pacific), and their pattern correlation coefficient is 0.625. Figure 10b shows the anomalous southeasterlies over Japan and the westerlies in the tropics shown in the NEA wind pattern. Figure 10c is also similar to the MEA vorticity pattern (Figure 5c), with a pattern correlation coefficient of 0.764. In addition, the significant wind anomalies associated with MEA LTCs shown in the MEA wind pattern are evident and statistically significant in Figure 10d. The pattern correlation coefficient between Figure 10e and the SEA vorticity pattern (Figure 6a) is 0.761, indicating that the relationship between circulation and SEA TC landfalls was reflected well by the SDTFM. Although not statistically significant, Figure 10f shows the wind features related to SEA

TABLE 3 Results of goodness-of-fit measures of the potential predictors for each domain

Domain	Predictors	RMSE	R^2	*F*_ratio
NEA	x_1	1.67	0.14	6.00
	x_2	1.70	0.11	4.63
	$\mathbf{x_1,x_2}$	**1.49**	**0.34**	**9.28**
MEA	x_1	1.18	0.13	5.59
	$\mathbf{x_2}$	**1.14**	**0.18**	**8.27**
	x_1,x_2	1.14	0.20	4.60
SEA	x_1	2.23	0.11	4.53
	x_2	2.15	0.17	7.79
	$\mathbf{x_1,x_2}$	**1.97**	**0.32**	**8.64**
EEA	$\mathbf{x_1}$	**1.84**	**0.20**	**9.36**
	x_2	1.92	0.13	5.42
	x_1,x_2	1.82	0.24	5.65

Note: Bold means that it is selected as the final predictor.

TABLE 2 Potential predictors that could be used in the statistical-dynamical seasonal typhoon forecast model (SDTFM) for each domain

Domain	Atmospheric variable	x_1	x_2
NEA	500 hPa vorticity	27–32°N 109–115°E	10–15°N 138–145°E
MEA	700 hPa vorticity	21–32°N 110–115°E	49–54°N 140–150°E
SEA	500 hPa vorticity	38–43°N 110–118°E	13–18°N 96–104°E
EEA	500 hPa vorticity	10–18°N 93–98°E	2–6°N 102–109°E

LTCs, such as the anomalous northwesterlies over Japan and the anomalous easterlies near 20°N. Figure 10g is also similar to the EEA vorticity pattern (Figure 7a) (e.g., negative vorticity around 40°N, and positive vorticities around 20°N), with a pattern correlation coefficient at 0.737. Figure 10h shows the anomalous subtropical easterlies and the anomalous tropical westerlies, which are similar to the EEA wind pattern (Figure 7c) and are statistically significant. These results indicate that the PNU CGCM performs well in predicting the observed spatial–temporal relationship of TC landfalls with atmospheric circulation, despite the spatial shift in the position of the major vortices shown in Figure 8 (Sun and Ahn, 2011).

TABLE 4 SDTFM for each domain

Domain	SDTFM
NEA	$y = 4.872 + 0.872x_1 + 0.816x_2$
MEA	$y = 3.359 - 0.526x_2$
SEA	$y = 8.308 + 0.900x_1 - 1.076x_2$
EEA	$y = 11.128 - 0.900x_1$

6 | COMPARING WITH OTHER FORECASTS

This study produces improved the prediction results compared to existing studies. As mentioned in Section 1, Sun and Ahn (2011) predicted the TC landfalls in south China from 1979 to 2009, with the same CGCM with lower versions. The period of our study was 1980–2018, and the predicted region covered the whole of EA, so the spatial–temporal range was wider than Sun and Ahn (2011). In addition, they used the initial conditions of July, but the current models predicted LTCs earlier than theirs using the initial conditions of May. Zhang *et al*. (2017) predicted the LTCs for NEA, MEA, SEA, and EEA using the initial conditions from January to June. The hybrid model developed by them used 4–5 predictors for each domain, with different initial conditions for each predictor. In comparison, our model was simple because only one initial condition was used to compute the predictors. Tian and Fan (2019) predicted the TC landfalls in China during June–July–August using relative vorticity as a predictor. In China, typhoons land more frequently in September than in June (Figure 2b,c), but September was excluded from their forecast season. The season in

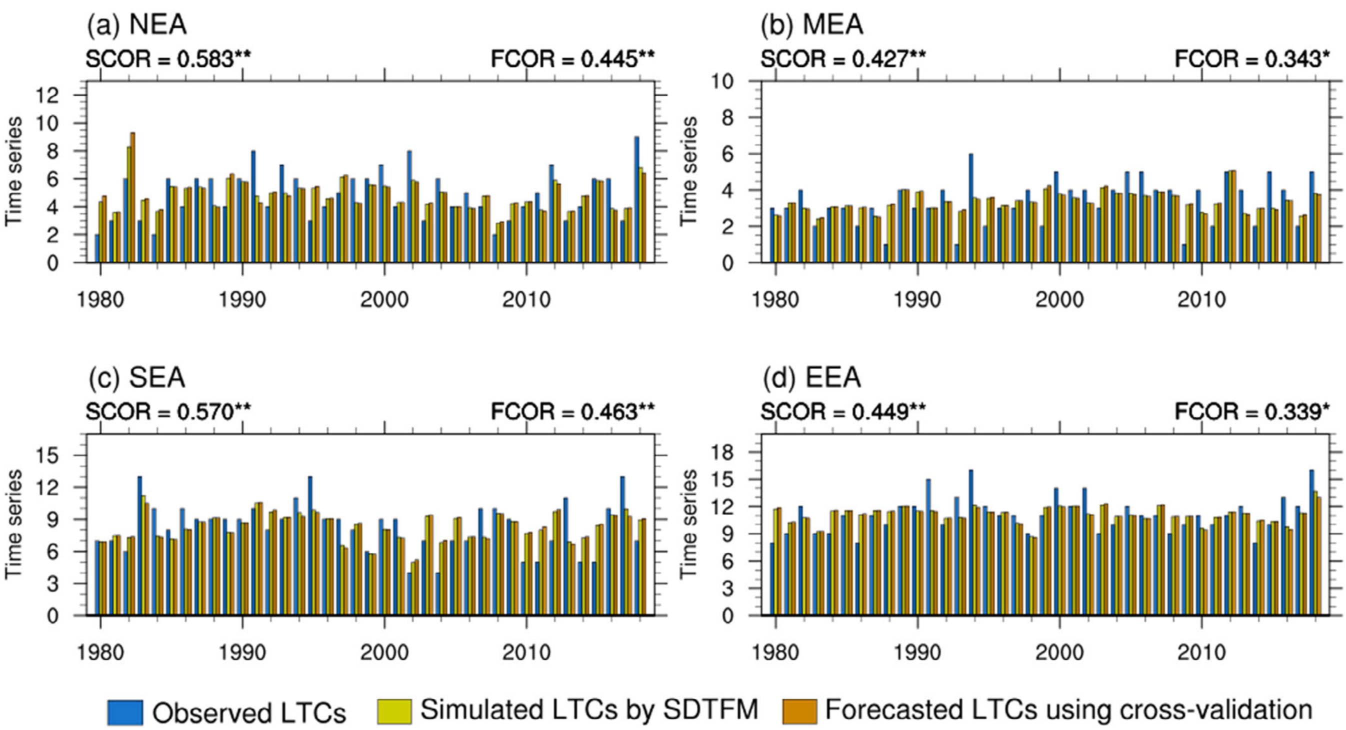

FIGURE 9 Time series of the observed TC landfalls, the simulated TC landfalls from the SDTFM, and the forecast TC landfalls from the SDTFM using leave-one-out cross-validation (LOOCV) for the 1980–2018 period over (a) NEA, (b) MEA, (c) SEA, and (d) EEA. SCOR (FCOR) are the correlation coefficients between the observed TC landfalls and the simulated (forecast) TC landfalls for every year from 1980 to 2018. * and ** indicate the significance at the 95% and 99% confidence levels [Colour figure can be viewed at wileyonlinelibrary.com]

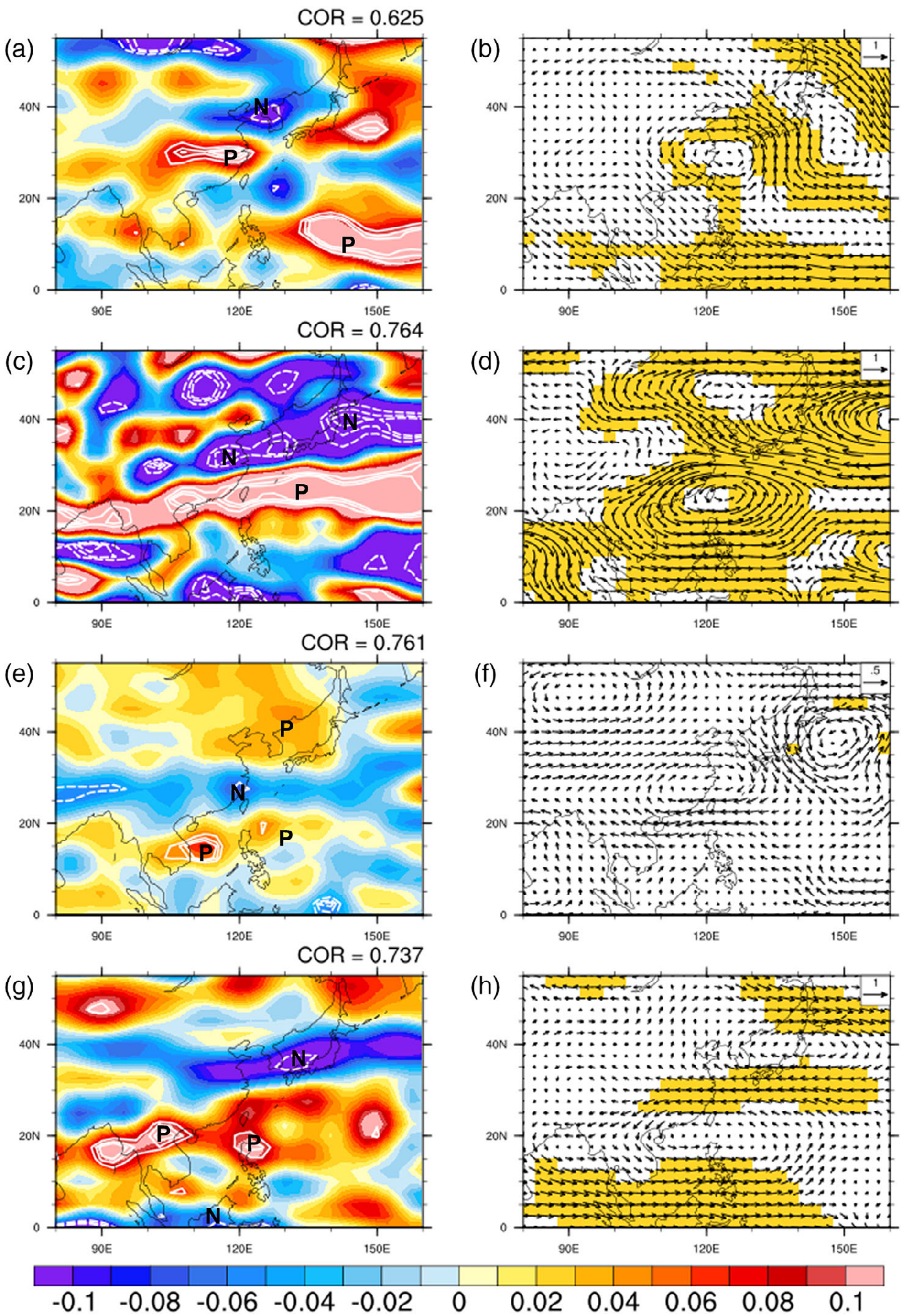

FIGURE 10 Regression of relative vorticity (left column) and horizontal wind (right column) at (a,b) 500 hPa, (c,d) 700 hPa, (e,f) 500 hPa, and (g,h) 500 hPa from R-2 onto the PNU-CGCM-predicted TC landfalls over (a,b) NEA, (c,d) MEA, (e,f) SEA, and (g,h) EEA for 1980–2018. In the left column, P (N) indicates positive (negative) vorticity, and the solid (dashed) lines indicate positively (negatively) significant areas at the 95%, 98%, and 99% confidence levels. COR is the spatial correlation with vorticity patterns for each domain. The shading in the right column indicates the areas at the 95% confidence level [Colour figure can be viewed at wileyonlinelibrary.com]

this study is JAS/JASON, which is more advantageous in predicting TCs during frequent typhoon landfalls.

7 | SUMMARY AND CONCLUSION

This study examines the correlation between TC landfall and atmospheric circulation, and based on that relationship, develops an SDTFM using the dynamic model and linear regression. LTCs in EA inflict serious economic and social damage on countries along the Western Pacific during boreal summer, and its landfall frequency during the TC season is gradually increasing in accordance with climate change, especially in the NEA, MEA and EEA (Figure S2). The long-term prediction of TC landfalls in EA is effective in minimizing such damage and is being continuously developed. The CGCM used in this study was PNU CGCM v2.0, which is a model participating in the APCC MME prediction system. The model produces a total of 40 ensemble members every month utilizing time-lag method, and SCM is used for ensemble prediction in this study. The SDTFMs are made for each of four regions: NEA, including the Korean Peninsula and Japan; MEA, including Taiwan, Fujian, Zhejiang, Jiangsu, and Shanghai; SEA, including South China, Vietnam, and the Philippines; and EEA. Tropical storms, severe tropical storms, and typhoons passing through each domain were defined as TC landfall. In addition, the predicted TC season was defined as JASON for SEA and JAS for the other domains, with more than 60% of TC landfalls occurring during this period.

To find appropriate predictors, the relationships between observed TC landfalls and mid- and low-level atmospheric circulation were analysed, and significant regression patterns were found in each domain. The NEA and MEA LTCs are affected by the anomalous subtropical easterlies and anomalous tropical westerlies. Such flow affects the low-level vorticity and vertical wind shear, inducing an environment favourable for TC generation and development. In particular, the anomalous subtropical easterlies determine the landing area, and the anomalous tropical westerlies prevent the TCs from entering SEA and help them move to the mid-latitudes. Meanwhile, the SEA LTCs are related to anomalous northwesterlies over Japan and anomalous easterlies at 20°N. They prevent TCs from moving to the mid-latitudes and allow them to land on SEA. In addition, the positive vorticity over the Philippine Sea provides an environment favourable for TC generation.

As a result of evaluating the potential of PNU-CGCM v2.0 to develop SDTFM, significant regression patterns were found for all domains when integrated with the May initial conditions. In the regression between the predicted relative vorticity and observed TC landfalls, the vorticities in significant areas were selected as potential predictors. Of three cases of potential predictors, the best-case was found by comparing the regression results while changing the predictors. The developed model offered significant predictions at the 99% confidence level for all domains. According to the LOOCV result, the SDTFM still predicted TC landfalls at the 99% confidence level for NEA and SEA, and 95% confidence level for MEA and EEA. That is, the SDTFM developed in this study can be used to predict TC landfalls in EA and its sub-domains.

ACKNOWLEDGEMENTS

This work was carried out with the support of the "Cooperative Research Program for Agriculture Science & Technology Development (Project No. PJ01489102)" Rural Development Administration, Republic of Korea.

AUTHOR CONTRIBUTIONS

So-Hee Kim: Data curation; formal analysis; investigation; methodology; software; visualization; writing – original draft. **Joong-Bae Ahn:** Conceptualization; funding acquisition; project administration; resources; supervision; validation; writing – review and editing. **Jianqi Sun:** Conceptualization; methodology.

ORCID

So-Hee Kim https://orcid.org/0000-0002-8179-2868
Joong-Bae Ahn https://orcid.org/0000-0001-6958-2801
Jianqi Sun https://orcid.org/0000-0002-3879-6986

REFERENCES

Ahn, J.-B. and Kim, H.-J. (2014) Improvement of 1-month lead predictability of the wintertime AO using a realistically varying solar constant for a CGCM. *Meteorological Applications*, 21(2), 415–418. https://doi.org/10.1002/met.1372F.

Ahn, J.-B. and Lee, J. (2016) A new multimodel ensemble method using nonlinear genetic algorithm: an application to boreal winter surface air temperature and precipitation prediction. *Journal of Geophysical Research: Atmospheres*, 121(16), 9263–9277. https://doi.org/10.1002/2016JD025151.

Ahn, J.-B., Lee, S.-B. and Ryoo, S.-B. (2012) Development of 12-month ensemble prediction system using PNU CGCM V1. 1. *Atmosphere*, 22(4), 455–464. https://doi.org/10.14191/Atmos.2012.22.4.455.

Bayasgalan, G. and Ahn, J.-B. (2018) Seasonal prediction of high-resolution temperature at 2-m height over Mongolia during boreal winter using both coupled general circulation model and artificial neural network. *International Journal of Climatology*, 38(14), 5418–5429. https://doi.org/10.1002/joc.5848.

Camp, J., Roberts, M., MacLachlan, C., Wallace, E., Hermanson, L., Brookshaw, A., Arribas, A. and Scaife, A.A. (2015) Seasonal forecasting of tropical storms using the Met Office GloSea5 seasonal forecast system. *Quarterly Journal of the Royal Meteorological Society*, 141(691), 2206–2219. https://doi.org/10.1002/qj.2516.

Chan, J.C.L. and Gray, W.M. (1982) Tropical cyclone movement and surrounding flow relationships. *Monthly Weather Review*, 110(10), 1354–1374. https://doi.org/10.1175/1520-0493(1982)110<1354:Tcmasf>2.0.Co;2.

Chan, J.C.L., Shi, J.-E. and Lam, C.-M. (1998) Seasonal forecasting of tropical cyclone activity over theWestern North Pacific and the South China Sea. *Weather and Forecasting*, 13(4), 997–1004. https://doi.org/10.1175/1520-0434(1998)013<0997:Sfotca>2.0.Co;2.

Chan, J.C.L., Shi, J.-E. and Liu, K. (2001) Improvements in the seasonal forecasting of tropical cyclone activity over the Western North Pacific. *Weather and Forecasting*, 16, 491–498. https://doi.org/10.1175/1520-0434(2001)016<0491:IITSFO>2.0.CO;2.

Chan, J.C.L. and Xu, M. (2009) Inter-annual and inter-decadal variations of landfalling tropical cyclones in East Asia. Part I: time series analysis. *International Journal of Climatology*, 29(9), 1285–1293. https://doi.org/10.1002/joc.1782.

Choi, K.-S. and Moon, I.-J. (2012) Changes in tropical cyclone activity that has affected Korea since 1999. *Natural Hazards*, 62, 971–989. https://doi.org/10.1007/s11069-012-0131-7.

Choi, K.-S., Park, K.-J., Lee, K.-M., Kim, J.-Y. and Kim, B.-J. (2015) Possible influence of Western North Pacific monsoon on tropical cyclone activity around Korea (in Korean with English abstract). *Journal of the Korean Earth Science Society*, 36(1), 68–81. https://doi.org/10.5467/JKESS.2015.36.1.68.

Choi, K.-S., Wu, C.-C. and Cha, E.-J. (2010a) Change of tropical cyclone activity by Pacific-Japan teleconnection pattern in the western North Pacific. *Journal of Geophysical Research: Atmospheres*, 115(D19), 1–13. https://doi.org/10.1029/2010jd013866.

Choi, W., Ho, C.-H. and Kim, H.-S. (2010b) Influence of large-scale environments on tropical cyclone activity over the Western North Pacific: a case study for 2009 (in Korean with English abstract). *The Korean Society of Climate Change Research*, 1(2), 133–145.

Chu, P.-S., Zhao, X., Lee, C.-T. and Lu, M.-M. (2007) Climate prediction of tropical cyclone activity in the vicinity of Taiwan using the multivariate least absolute deviation regression method. *Terrestrial Atmospheric and Oceanic Sciences*, 18(4), 805. https://doi.org/10.3319/TAO.2007.18.4.805(A).

Fan, K. (2007) North Pacific sea ice cover, a predictor for the Western North Pacific typhoon frequency? *Science in China Series D: Earth Sciences*, 50(8), 1251–1257. https://doi.org/10.1007/s11430-007-0076-y.

Fan, K. (2010) A prediction model for Atlantic named storm frequency using a year-by-year increment approach. *Weather and Forecasting*, 25(6), 1842–1851. https://doi.org/10.1175/2010waf2222406.1.

Fan, K. and Wang, H. (2009) A new approach to forecasting typhoon frequency over the Western North Pacific. *Weather and Forecasting*, 24(4), 974–986. https://doi.org/10.1175/2009waf2222194.1.

Harr, P.A. and Elsberry, R.L. (1991) Tropical cyclone track characteristics as a function of large-scale circulation anomalies. *Monthly Weather Review*, 119(6), 1448–1468. https://doi.org/10.1175/1520-0493(1991)119<1448:Tctcaa>2.0.Co;2.

Harr, P.A. and Elsberry, R.L. (1995) Large-scale circulation variability over the tropical Western North Pacific. Part I: Spatial patterns and tropical cyclone characteristics. *Monthly Weather Review*, 123(5), 1225–1246. https://doi.org/10.1175/1520-0493(1995)123<1225:Lscvot>2.0.Co;2.

Huang, W.-R. and Chan, J.C.L. (2014) Dynamical downscaling forecasts of Western North Pacific tropical cyclone genesis and landfall. *Climate Dynamics*, 42(7), 2227–2237. https://doi.org/10.1007/s00382-013-1747-3.

IPCC. (2014) Climate change 2014: synthesis report. In: Pachauri, R.K. and Meyer, L.A. (Eds.) *Contribution of Working Groups I, II and III to the Fifth Assessment Report of the Intergovernmental Panel on Climate Change*. Geneva, Switzerland: IPCC. 151 pp.

IPCC. (2019) Summary for policymakers. In: Pörtner, H.-O., Roberts, D.C., Masson-Delmotte, V., Zhai, P., Tignor, M., Poloczanska, E., Mintenbeck, K., Nicolai, M., Okem, A., Petzold, J., Rama, B. and Weyer, N. (Eds.) *IPCC Special Report on the Ocean and Cryosphere in a Changing Climate*, (in press). IPCC.

Jeong, H.-I., Ashok, K., Song, B.G. and Min, Y.M. (2008) Experimental 6-month hindcast and forecast simulation using CCSM3. In: *APCC 2008 Technical Report*. South Korea: APEC Climate Center.

Jo, S. and Ahn, J.-B. (2015) Improvement of CGCM prediction for wet season precipitation over maritime continent using a bias correction method. *International Journal of Climatology*, 35(13), 3721–3732. https://doi.org/10.1002/joc.4232.

Kanamitsu, M., Ebisuzaki, W., Woollen, J., Yang, S., Hnilo, J., Fiorino, M. and Potter, G. (2002) *NCEP-DEO AMIP-II Reanalysis (R-2)*. U.S.A.: Bul. of the Atmos. Met. Soc, pp. 1631–1643.

Kim, G., Ahn, J.-B., Kryjov, V.N., Lee, W.-S., Kim, D.-J. and Kumar, A. (2021) Assessment of MME methods for seasonal prediction using WMO LC-LRFMME hindcast dataset. *International Journal of Climatology*, 41(S1), E2462–E2481. https://doi.org/10.1002/joc.6858.

Kim, H.-M., Chang, E.K.M. and Zhang, M. (2015) Statistical–dynamical seasonal forecast for tropical cyclones affecting New York state. *Weather and Forecasting*, 30(2), 295–307. https://doi.org/10.1175/waf-d-14-00089.1.

Kim, J., Ho, C., Kim, H., Sui, C. and Park, S.K. (2008) Systematic variation of summertime tropical cyclone activity in the Western North Pacific in relation to the madden–Julian oscillation. *Journal of Climate*, 21(6), 1171–1191. https://doi.org/10.1175/2007JCLI1493.1.

Kim, J.-S., Yoon, S.-K., Moon, Y.-I. and Lee, J.-H. (2012) Atmospheric circulation of Pacific-Japan (PJ) and typhoon-induced extremes in the Nakdong River Basin (in Korean with English abstract). *Journal of Korea Water Resources Association*, 45(12), 1309–1319. https://doi.org/10.3741/JKWRA.2012.45.12.1309.

Kim, O.-Y., Kim, H.-M., Lee, M.-I. and Min, Y.-M. (2017) Dynamical–statistical seasonal prediction for western North Pacific typhoons based on APCC multi-models. *Climate Dynamics*, 48(1), 71–88. https://doi.org/10.1007/s00382-016-3063-1.

Lee, S.-M., Kang, H.-S., Kim, Y.-H., Byun, Y.-H. and Cho, C. (2016) Verification and comparison of forecast skill between global seasonal forecasting system version 5 and unified model during 2014 (in Korean with English abstract). *Atmosphere*, 26(1), 59–72. https://doi.org/10.14191/Atmos.2016.26.1.059.

Lee, T.-C., Knutson, T.R., Kamahori, H. and Ying, M. (2012) Impacts of climate change on tropical cyclones in the Western North Pacific Basin. Part I: Past observations. *Tropical Cyclone Research and Review*, 1(2), 213–235. https://doi.org/10.6057/2012TCRR02.08.

Li, X., Yang, S., Wang, H., Jia, X. and Kumar, A. (2013) A dynamical-statistical forecast model for the annual frequency of western Pacific tropical cyclones based on the NCEP climate forecast system version 2. *Journal of Geophysical Research: Atmospheres*, 118(21), 12,061–12,074. https://doi.org/10.1002/2013jd020708.

Liu, K.S. and Chan, J.C.L. (2003) Climatological characteristics and seasonal forecasting of tropical cyclones making landfall along the South China Coast. *Monthly Weather Review*, 131(8 PART 1), 1650–1662. https://doi.org/10.1175//2554.1.

Min, Y.M., Kryjov, V.N. and Oh, S.M. (2014) Assessment of APCC multimodel ensemble prediction in seasonal climate forecasting: retrospective (1983–2003) and real-time forecasts (2008–2013). *Journal of Geophysical Research: Atmospheres*, 119(21), 12,132–112,150. https://doi.org/10.1002/2014JD022230.

Mori, N. and Takemi, T. (2016) Impact assessment of coastal hazards due to future changes of tropical cyclones in the North Pacific Ocean. *Weather and Climate Extremes*, 11, 53–69. https://doi.org/10.1016/j.wace.2015.09.002.

Murakami, H., Villarini, G., Vecchi, G.A., Zhang, W. and Gudgel, R. (2016) Statistical–dynamical seasonal forecast of North Atlantic and U.S. landfalling tropical cyclones using the high-resolution GFDL FLOR coupled model. *Monthly Weather Review*, 144(6), 2101–2123. https://doi.org/10.1175/mwr-d-15-0308.1.

Oh, S.-G. and Suh, M.-S. (2017) Comparison of projection skills of deterministic ensemble methods using pseudo-simulation data generated from multivariate Gaussian distribution. *Theoretical and Applied Climatology*, 129(1–2), 243–262. https://doi.org/10.1007/s00704-016-1782-1.

Park, D.-S.R., Ho, C.-H., Kim, J.-H. and Kim, H.-S. (2011) Strong landfall typhoons in Korea and Japan in a recent decade. *Journal of Geophysical Research: Atmospheres*, 116(D7), 1–11. https://doi.org/10.1029/2010jd014801.

Seong, M.-G., Suh, M.-S. and Kim, C. (2017) Intercomparison of prediction skills of ensemble methods using monthly mean temperature simulated by CMIP5 models. *Asia-Pacific Journal of Atmospheric Sciences*, 53(3), 339–351. https://doi.org/10.1007/s13143-017-0039-y.

Sparks, N. and Toumi, R. (2021) On the seasonal and sub-seasonal factors influencing East China tropical cyclone landfall. *Atmospheric Science Letters*, 22(2), e1014. https://doi.org/10.1002/asl.1014.

Sun, J. and Ahn, J.B. (2011) A GCM-based forecasting model for the landfall of tropical cyclones in China. *Advances in Atmospheric Sciences*, 28(5), 1049–1055. https://doi.org/10.1007/s00376-011-0122-8.

Tian, B. and Fan, K. (2019) Seasonal climate prediction models for the number of landfalling tropical cyclones in china. *Journal of Meteorological Research*, 33(5), 837–850. https://doi.org/10.1007/s13351-019-8187-x

Tu, J.-Y., Chou, C. and Chu, P.-S. (2009) The abrupt shift of typhoon activity in the vicinity of Taiwan and its association with Western North Pacific-East Asian climate change. *Journal of Climate*, 22(13), 3617–3628. https://doi.org/10.1175/2009jcli2411.1.

Vecchi, G.A. and Villarini, G. (2014) Next season's hurricanes. *Science*, 343(6171), 618–619. https://doi.org/10.1126/science.1247759.

Vecchi, G.A., Zhao, M., Wang, H., Villarini, G., Rosati, A., Kumar, A., Held, I.M. and Gudgel, R. (2011) Statistical–dynamical predictions of seasonal North Atlantic hurricane activity. *Monthly Weather Review*, 139(4), 1070–1082. https://doi.org/10.1175/2010mwr3499.1.

Vitart, F. and Stockdale, T.N. (2001) Seasonal forecasting of tropical storms using coupled GCM integrations. *Monthly Weather Review*, 129(10), 2521–2537. https://doi.org/10.1175/1520-0493(2001)129<2521:Sfotsu>2.0.Co;2.

Wang, B. and Chan, J.C.L. (2002) How strong ENSO events affect tropical storm activity over the Western North Pacific. *Journal of Climate*, 15(13), 1643–1658. https://doi.org/10.1175/1520-0442(2002)015<1643:Hseeat>2.0.Co;2.

Wang, B. and Fan, Z. (1999) Choice of South Asian summer monsoon indices. *Bulletin of the American Meteorological Society*, 80(4), 629–638.

Wang, B., Xiang, B. and Lee, J.-Y. (2013) Subtropical high predictability establishes a promising way for monsoon and tropical storm predictions. *Proceedings of the National Academy of Sciences*, 110(8), 2718–2722. https://doi.org/10.1073/pnas.1214626110.

Wang, H., Scheme, J.K.E., Kumar, A., Wang, W., Long, L., Chelliah, M., Bell, G.D. and Peng, P. (2009) A statistical forecast model for Atlantic seasonal hurricane activity based on the NCEP dynamical seasonal forecast. *Journal of Climate*, 22, 4481–4500.

Weigel, A.P., Liniger, M.A. and Appenzeller, C. (2008) Can multi-model combination really enhance the prediction skill of probabilistic ensemble forecasts? *Quarterly Journal of the Royal Meteorological Society*, 134(630), 241–260. https://doi.org/10.1002/qj.210.

Wilks, D.S. (2006) *Statistical Methods in the Atmospheric Sciences. International Geophysics Series*, Vol. 91, 2nd edition. U.S.A.: Academic Press, p. 627.

Xiang, B., Lin, S.-J., Zhao, M., Zhang, S., Vecchi, G., Li, T., Jiang, X., Harris, L. and Chen, J.-H. (2015) Beyond weather time-scale prediction for hurricane sandy and super typhoon Haiyan in a global climate model. *Monthly Weather Review*, 143(2), 524–535. https://doi.org/10.1175/mwr-d-14-00227.1.

Zhang, W., Leung, Y. and Chan, J.C.L. (2013) The analysis of tropical cyclone tracks in the Western North Pacific through data mining. Part I: Tropical cyclone recurvature. *Journal of Applied Meteorology and Climatology*, 52(6), 1394–1416. https://doi.org/10.1175/jamc-d-12-045.1.

Zhang, W., Vecchi, G.A., Villarini, G., Hiroyuki, M., Gudgel, R. and Xiaosong, Y. (2017) Statistical–dynamical seasonal forecast of Western North Pacific and East Asia landfalling tropical cyclones using the GFDL FLOR coupled climate model. *Journal of Climate*, 30(6), 2209–2232. https://doi.org/10.1175/JCLI-D-16-0487.1.

Zhang, W., Villarini, G., Vecchi, G.A., Murakami, H. and Gudgel, R. (2016) Statistical-dynamical seasonal forecast of western North Pacific and East Asia landfalling tropical cyclones using the high-resolution GFDL FLOR coupled model. *Journal of Advances in Modeling Earth Systems*, 8(2), 538–565. https://doi.org/10.1002/2015ms000607.

Zhao, M., Held, I.M. and Vecchi, G.A. (2010) Retrospective forecasts of the hurricane season using a global atmospheric model assuming persistence of SST anomalies. *Monthly Weather Review*, 138(10), 3858–3868. https://doi.org/10.1175/2010mwr3366.1.

SUPPORTING INFORMATION

Additional supporting information may be found in the online version of the article at the publisher's website.

How to cite this article: Kim, S.-H., Ahn, J.-B., & Sun, J. (2021). Dynamical-statistical long-term prediction for tropical cyclone landfalls in East Asia. *International Journal of Climatology*, 1–15. https://doi.org/10.1002/joc.7382